J|A|C|S
ARTICLES
Published on Web 02/25/2006

On the Affinity Regulation of the Metal-Ion-Dependent Adhesion Sites in Integrins

Eider San Sebastian,[†] Jose M. Mercero,[†] Roland H. Stote,[‡] Annick Dejaegere,[§] Fernando P. Cossío,*[,†] and Xabier Lopez*[,†]

Contribution from the Kimika Fakultatea, Euskal Herriko Unibertsitatea and Donostia International Physics Center (DIPC), P. K. 1072, 20080 Donostia, Spain, Laboratoire de Biophysicochimie Moléculaire, UMR Chimie Physique Moléculaire et Spectroscopie, Université Louis Pasteur, Strasbourg, France, and UMR 7104 Biocomputing Group, Structural Biology & Genomics Department, Ecole Supérieure de Biotechnologie de Strasbourg-IGBMC; BP 10413 - F- 67412 Illkirch, France

Received June 23, 2005; E-mail: fp.cossio@ehu.es; xabier.lopez@ehu.es

Abstract: Density functional theory and a polarizable continuum model are used to (i) understand the affinity modulating mechanisms of the interaction between the metal-ion-dependent adhesion site (MIDAS) of a selected integrin, lymphocyte function-associated antigen-1 (LFA-1) and a ligand mimetic acetate molecule and to (ii) propose a new, promising family of inhibitors to block the interaction of the integrin with intercellular adhesion molecule-1 (ICAM-1). We quantify the effect of isolated factors, such as the metal coordination, the nature of the ligand or the cation present on the MIDAS, and the effect of the permittivity of the media. We show that the affinity for ligand decreases when metal coordination changes from the *open* conformation to the *closed* conformation. In addition, Mn^{2+} and Zn^{2+} showed to be good competitors for the octahedrically coordinated Mg^{2+} and yielded excellent affinity values, whereas Ca^{2+} in an octahedric environmet would decrease the affinity for the ligand. Our affinity studies of the open MIDAS showed that nitronate-derived or carboxylic acid-containing ligands may represent new promising scaffolds of future inhibitors. Finally, we show that affinities are always highly favored by low-dielectric environments, which explains the propensity of MIDAS motifs to be surrounded by hydrophobic residues in integrins and highlights the importance of including hydrophobic groups in the inhibitors.

Introduction

Protein−protein interactions determine the course of many biologically important processes. In particular, interactions between proteins of the integrin family and cell adhesion molecules (CAMs) are central to a variety of phenomena, including embryonic cell migration, wound healing, immune responses, and cancer metastasis.[1−3] Lymphocyte function-associated antigen-1 (LFA-1, $\alpha L\beta 2$) is an integrin mainly confined to leukocytes, which binds to the intercellular adhesion molecule-1 (ICAM-1) located on neighboring endothelial cells via a particular fragment called the inserted domain (I-domain) (Figure 1A), playing a key role in inflammatory diseases and cancer metastasis.[4]

Key aspects of the affinity and specificity of this interaction have been addressed by combining the available atomic-resolution structural information for the I-domain of LFA-1 and ICAM-1 with a broad range of biochemical data.[5−8] A Mg^{2+} ion at the "top" of the I-domain coordinates to E34 in ICAM-1; this Mg^{2+} ion and the residues to which it is coordinated constitute the metal-ion-dependent adhesion site (MIDAS),[9] which has been chosen for study in this work.

From crystallographic analysis, it is known that the MIDAS motif can adopt two alternative conformations, referred to as *open* and *closed*. In both conformations, the metal coordinates octahedrically to six polar residues, following the coordination pattern observed for this cation in proteins.[10,11] In the closed conformation, the metal ion binds to one aspartate (D137) and two serines (S139, S141); three water molecules (Figure 2B) complete the coordination sphere. In the open MIDAS conformation, the metal ion binds two serines (S139, S141), one threonine (T206), and two water molecules. In the crystal-

[†] Euskal Herriko Unibertsitatea and Donostia International Physics Center.
[‡] Universit Louis Pasteur.
[§] Ecole Supérieure de Biotechnologie de Strasbourg-IGBMC.

(1) Aplin, A. E.; Howe, A. K.; Juliano, R. L. *Curr. Opin. Cell Biol.* **1999**, *11*, 737−744.
(2) Plow, E. F.; Haas, T. A.; Zhang, L.; Loftus, J.; Smith, J. W. *J. Biol. Chem.* **2000**, *275*, 21785−21788.
(3) Gottschalk, K.-E.; Kessler, H. *Angew. Chem., Int. Ed.* **2002**, *20*, 3767−3774.
(4) Larson, R. S.; Springer, T. A. *Immunol. Rev.* **1990**, *114*, 181−216.
(5) Huang, C.; Springer, T. A. *J. Biol. Chem.* **1995**, *270*, 19008−19016.
(6) Stanley, P.; Hogg, N. *J. Biol. Chem.* **1998**, *273*, 3358−3362.
(7) Shimaoka, M.; Xiao, T.; Liu, J. H.; Yang, Y.; Dong, Y.; Jun, C. D.; McCormack, A.; Zhang, R.; Joachimiak, A.; Takagi, J.; Wang, J.-H.; Springer, T. A. *Cell* **2003**, *112*, 99−111.
(8) Song, G.; Yang, Y.; Liu, J.-h.; Casasnovas, J. M.; Shimaoka, M.; Springer, T. A.; Wang, J.-h. *PNAS* **2005**, *9*, 3366−3371.
(9) Lee, J.-O.; Rieu, P.; Arnaout, M. A.; Liddington, R. C. *Cell* **1995**, *80*, 631−638.
(10) Dudev, T.; Lim, C. *Chem. Rev.* **2003**, *103*, 773−787.
(11) Mayaan, E.; Range, K.; York, D. M. *J. Biol. Inorg. Chem.* **2004**, *9*, 807−817.

10.1021/ja054142a CCC: $33.50

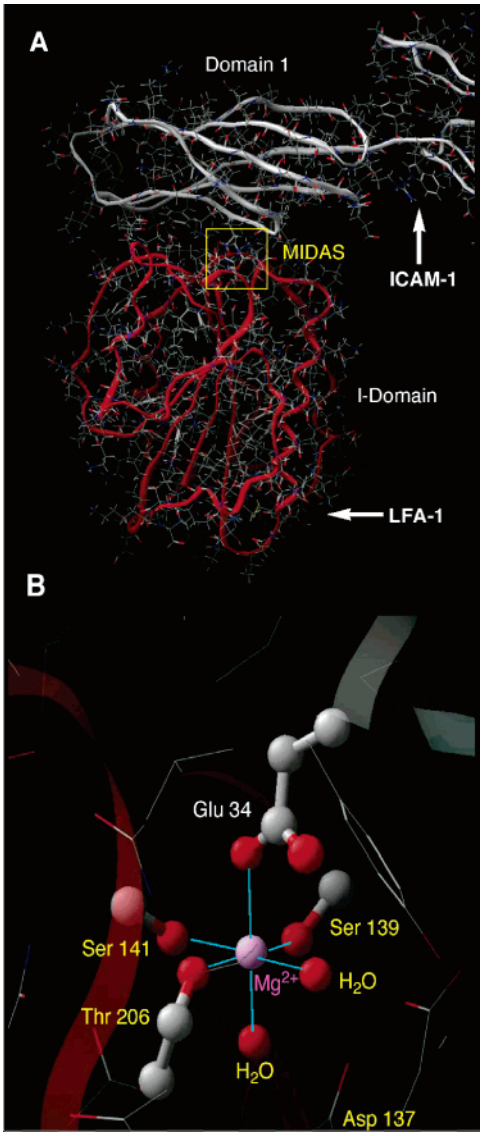

Figure 1. (A) Ribbon representation of the X-ray structure of the medium affinity conformation of the I-domain in LFA-1 (red), interacting with ICAM-1 (white) (PDB ID: 1mq8).[7] (B) Highlighted, the MIDAS motif (open state) in a ball-and-stick representation, where GLU-34 of ICAM-1 completes the coordination sphere of the metal.

lographic environment, a Glu residue from a neighboring I domain in the crystal lattice[9] or a Glu belonging to ICAM-1[7] (Figure 2A) also binds to the MIDAS. This suggests that when ICAM-1 binds to the I-domain (Figure 1A), one of the water molecules of the MIDAS is displaced by E34 in ICAM-1 (Figure 1B), and the latter becomes part of the metal-ion coordination sphere.[7] The binding of a Glu residue either from ICAM-1 or from a neighboring I-domain appears to be correlated with a change in conformation from the closed to the open form. These data suggest that the closed MIDAS conformation is present in inactivated LFA-1, with low affinity values toward ICAM-1. The open MIDAS conformation would be present in activated integrins, which show a higher affinity for the ligand. Thus, this change in the coordination of the MIDAS is believed to be one of the mechanisms that modulates the affinity of LFA-1 toward ICAM-1.[12]

Besides the role of conformational changes of the MIDAS in affinity modulation, it has also been established that integrin/

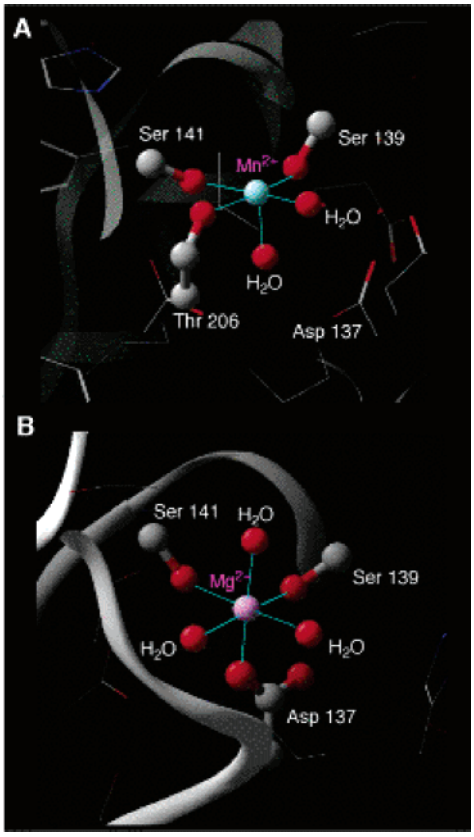

Figure 2. (A) Ball and stick representation of the open conformation of the MIDAS motif (from PDB ID: 1MQ9).[7] For the subsequent calculations, the original Mn^{2+} cation was replaced by Mg^{2+} and the sixth ligand (absent at the upper axial position in Fig. 1A), which was a Glu from a neighboring I-domain in the crystal lattice, was replaced by a water molecule to complete the octahedral coordination to the metal (See Figures 3 and 4 for the resultant coordination models). (B) Ball and stick representation of the closed conformation of the MIDAS motif (from PDB ID: 1MJN).[7]

ligand interactions depend strongly on the nature of divalent cations, such as Mg^{2+}.[6,13−15] Changes in integrin/ligand affinity have been observed as a function of other cations, such as Zn^{2+}, Ca^{2+}, and Mn^{2+}, but their binding site(s) and possible role(s) have not been unequivocally established. X-ray structures have confirmed the presence of a Mg^{2+} cation in the closed MIDAS motif[15] and a Mg^{2+} or a Mn^{2+} cation in the open MIDAS motif.[7,16] The role of Ca^{2+} cation on integrin activity, with controversial experimental results, has been widely discussed to date. Biochemical assays with isolated I-domains have suggested that Ca^{2+} is likely to bind differently in closely related I-domains, such as those of LFA-1 and Mac-1; these two I-domains have equivalent MIDAS motifs.[17] On the other hand, the effects of Ca^{2+} on the ligand binding have also been shown to vary as a function of concentration.[13−15,18−20] In addition, at

(12) Lu, C.; Shimaoka, M.; Oxvig, M.; Takagi, J.; Springer, T. A. *Proc. Natl. Acad. Sci. U.S.A.* **2001**, *98*, 2387−2392.
(13) Labadia, M. E.; Jeanfavre, D. D.; Caviness, G. O.; Morelock, M. M. *J. Immunol.* **1998**, *161*, 836−842.
(14) Dransfield, I.; Cabanas, C.; Craig, A.; Hogg, N. *J. Cell Biol.* **1992**, *116*, 219−226.
(15) Qu, A.; Leahy, D. J. *Structure* **1996**, *4*, 931−942.
(16) Qu, A.; Lehaly, D. *Proc. Natl. Acad. Sci. U.S.A.* **1995**, *92*, 10277−10281.
(17) Griggs, D. W.; Schmidt, C. M.; Carron, C. P. *J. Biol. Chem.* **1998**, *273*, 22113−22119.
(18) Chateau, M.; Chen, S.; Salas, A.; Springer, T. A. *Biochemistry* **2001**, *40*, 13972−13979.
(19) Lu, C.; Shimaoka, M.; Znag, Q.; Takagi, J.; Springer, T. A. *Proc. Natl. Acad. Sci. U.S.A.* **2001**, *98*, 2393−2398.
(20) Xiong, Y. M.; Zhang, L. *J. Biol. Chem.* **2001**, *276*, 19340−19349.

least a high and a low affinity Ca^{2+} binding motifs have been characterized so far, but not unequivocally localized, in intact LFA-1.[13,17] All these features of integrins make it difficult to unequivocally assign a role to Ca^{2+}. On the other hand, to the best of our knowledge, little is known about the effect of the Zn^{2+} cation on LFA-1/ICAM-1 binding. According to Griggs and co-workers,[17] Zn^{2+} can bind to isolated I-domains of LFA-1 and Mac-1, which have a single and identical MIDAS motif, whereas Novick et al.[21] assigned an antiinflammatory role to Zn^{2+} and proposed that this effect was due to a direct blocking of the interaction between LFA-1 and ICAM-1 but did not establish a direct coordination of Zn^{2+} metal to the MIDAS motif.

The ambiguous interpretation concerning the role of metal ions in integrin/ligand interactions is, in part, due to the difficulty in isolating the direct effect of metal coordination on ligand binding from many other factors,[22] such as conformational effects, the existence of several metal binding sites, or different experimental conditions. In the present work, we used state of the art quantum calculations to establish the intrinsic preference of the metal binding site (MIDAS) in its closed and open conformations for the cations Mg^{2+}, Mn^{2+}, Zn^{2+}, and Ca^{2+} and to quantify the differential ability of these metals to promote ligand binding on the open MIDAS motif.

The administration of small inhibitors that bind specifically and effectively to the I-domain, thus blocking the binding of LFA-1 to ICAM-1, constitutes an efficient tool for fighting against the pathologies mentioned earlier. In the interest of designing novel families of antimetastatic and antiimflammatory drugs,[23] an understanding of the binding modes and affinity regulation at a molecular level is needed. With this purpose in mind, new ligand types were tested for their binding affinities to the MIDAS using quantum mechanical calculations. These ligands could eventually serve as scaffolds for new inhibitory compounds, which could complement those inhibitors already developed based mostly on the geometric and electronic features of the active site of ICAM-1.[24] In addition, previous studies[10] suggest that local hydrophobic environments can substantially modify the protein−protein interaction equilibria. With this in mind, we analyzed the effect of different dielectric permittivity values on the binding of the ligands to the MIDAS complexes, results which should be applied to the design of inhibitory drugs.

In this work, then, five different aspects of the LFA-1/ICAM-1 interaction were studied by Density Functional Theory (DFT) calculations: (i) variation of the affinity energies of the Mg^{2+}-bound MIDAS toward an acetate, as a consequence of changes in the coordination of the metal (closed vs open), (ii) competition/interchange of cations of diverse nature in both the open and closed MIDAS, iii) variation of the affinity of the open MIDAS motif toward the incoming ligand (an acetate molecule), as a function of the metal ion, (Mg^{2+}, Ca^{2+}, Zn^{2+} and Mn^{2+}), iv) influence of the nature of the incoming ligand on its binding affinity to the Mg^{2+}-bound open MIDAS motif and v) effect of the dielectric permittivity of the environment on the binding energies.

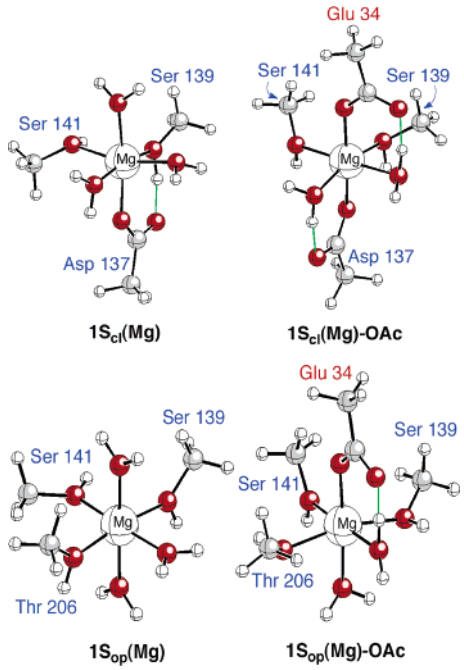

Figure 3. Ball and stick representation of the MIDAS motif with first-shell residues. Top: the closed conformation in the absence (left) or presence (right) of GLU-34 from ICAM-1. Bottom: open conformation in the absence (left) or presence (right) of GLU-34 from ICAM-1.

Methods

Preparation of the Structures. Initial geometries for the different MIDAS complexes studied in this work were obtained from molecular dynamics (MD) simulations of the following X-ray structures (PDB ID are given), available in the Protein Data Bank (www.rcsb.org/pdb/):[25] 1MJN for the water-bound closed MIDAS (Figures 3 and 4, top, left.), 1MQ9 for the open MIDAS in the ligand-free I-domain (Figures 3 and 4, bottom, left), and 1MQ8 for the open MIDAS in the ligand bound I-domain, (Figures 3 and 4, bottom, right). As there is no entry to date for a crystal structure of a closed MIDAS bound to ICAM-1, 1MJN and 1MQ9 were combined to obtain the remaining starting geometries (Figures 3 and 4, top, right). In 1MJN and 1MQ8, the metal cation in the MIDAS motif is Mg^{2+}, whereas that in 1MQ9 is Mn^{2+}. In the latter, we replaced Mn^{2+} by Mg^{2+} prior to running the MD simulations. Molecular dynamics simulations were run by using the CHARMM program[26] with the all-atom protein force field.[27]

The hydrogen atoms were placed using the HBUILD facility of the CHARMM program,[28] and the system was energy minimized by 1000 steps using the Steepest Descent algorithm. The system was solvated with explicit waters, heated to 300 K, and equilibrated for 25 ps. From the equilibrated structures, first and second-shell residues around the Mg^{2+} were extracted for subsequent quantum mechanical calculations; i.e., amino acids and water molecules directly or indirectly coordinated to the metal were identified and isolated from the rest of the protein in the structure files. The primary objective of these short molecular dynamics simulations was to generate a set of reasonable initial structures for the quantum geometry optimizations. Some of these molecular dynamics have then been extended to cover nanosecond time scales. The details of these molecular dynamics simulations will be presented in more detail in a later publication. However, it is noteworthy to point out that along these simulations, there were not significant local conformational changes on the first coordination shell around the

(21) Novick, S. G.; Fodfrey, J. C.; Pollack, R. L.; Wilder, H. R. *Med. Hypotheses* **1997**, *49*, 347−357.
(22) Ajroud, K.; Sugimori, T.; Goldmann, W. H.; Fathallah, D. M.; Xiong, J.-P.; Arnaout, M. A. *J. Biol. Chem.* **2004**, *279*, 25483−25488.
(23) Zubia, A.; Mendoza, L.; Vivanco, S.; Albada, E.; Carrascal, T.; Lecea, B.; Arrieta, A.; Zimmerman, T.; Vidal-Vanaclocha, F.; Cossio, F. P. *Angew. Chem., Int. Ed.* **2005**, *44*, 2903−2907.
(24) Gadek, T. R. et al. *Science* **2002**, *295*, 1086−1089.
(25) Berman, H.; Westbrook, J.; Feng, Z.; Gilliland, G.; Bhat, T.; Weissig, H.; Shindyalov, I.; Bourne, P. *Nucleic Acids Res.* **2000**, *28*, 235−242.
(26) Brooks, B. R.; Bruccoleri, B. D.; Olafson, B. D.; States, D. J.; Swaminathan, S.; Karplus, M. *J. Comput. Chem.* **1983**, *4*, 187−217.
(27) Karplus, M. et al. *J. Phys. Chem. B* **1998**, *102*, 3586−3616.
(28) Brunger, A. T.; Karplus, M. *Proteins* **1988**, *4*, 148−156.

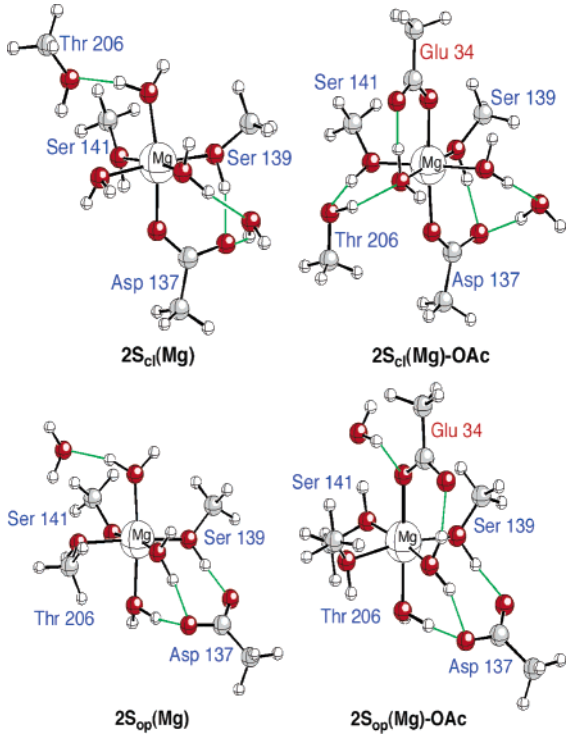

Figure 4. Ball and stick representation of the MIDAS motif with first and second-shell residues. Top: closed conformation in the absence (left) or presence (right) of GLU-34 from ICAM-1. Bottom: open conformation in the absence (left) or presence (right) of GLU-34 from ICAM-1.

Mg^{2+}, supporting our choice of structures for the present work. From these geometries, two sets of MIDAS model structures were built. In both sets, the minimal number of residues required to adequately reproduce the local features of the environment were used, and the remaining valences were saturated with hydrogen atoms; i.e, acetate was used instead of glutamate and aspartate, and methanol was used instead of serine and threonine. In the first set of structures, the MIDAS is represented by the six residues octahedrically coordinated to the cation, which complete the first coordination shell of the Mg^{2+}. The resultant structures for the closed and open MIDAS conformations are named $1S_{cl}$ (Figure 3, top) and $1S_{op}$ (Figure 3, bottom), respectively, where the subscripts refer to the closed and open conformations, and 1S stands for first shell. In the second set of structures, key second-shell ligands (amino acids and water molecules) were also included to build a more realistic model of the MIDAS as well as to take into better account the environmental changes that occur when passing from the closed to the open MIDAS conformation. For example, Asp-137 is present in the $1S_{cl}$ structure but absent in that of $1S_{op}$, when, in fact, it is displaced to the second shell of the metal in the open MIDAS conformation; a water molecule is also present in the second shell of the metal ion and thus absent in the 1S model. Similarly, Thr-206, present in $1S_{op}$ and absent in $1S_{cl}$, is also in the second coordination shell when the MIDAS is closed. Therefore, in the second set of structures, these residues were also included. These structures are denoted in this paper by $2S_{cl}$ (Figure 4, top) and $2S_{op}$ (Figure 4, bottom), respectively, where 2S stands for second shell.

Gas-Phase Results. The change in Gibbs free energy in the following type of equilibrium is estimated:

$$\text{(MIDAS)M}-\text{W} + \text{L} \xrightarrow{\Delta G^{s}_{aff}} \text{(MIDAS)M}-\text{L} + \text{W} \qquad (1)$$

$$\text{(MIDAS)Mg}-\text{W} + \text{M}-6\text{W}$$

$$\downarrow (\Delta G^{s}_{ex})$$

$$\text{(MIDAS)M}-\text{W} + \text{Mg}-6\text{W} \qquad (2)$$

where M stands for metal, L for ligand, W for water, ΔG^{s}_{aff} for the change in the Gibbs free energy of ligand binding in different solvents, and ΔG^{s}_{ex} for the change in Gibbs free energy for the cation exchange reaction in different solvents. These two equilibria summarize the reactions studied in this paper, and they will be discussed individually later in the text. Here, we note that the (MIDAS)M−W and (MIDAS)M−L terms in eqs 1 and 2 represent, respectively, water and ligand bound to the MIDAS motif, where M is one of the following metal ions: Mg^{2+}, Zn^{2+}, Ca^{2+}, or Mn^{2+}. The MIDAS motif is represented by the following models: $1S_{cl}$, $1S_{op}$, $2S_{cl}$, or $2S_{op}$. M−6W represents the hexahydrated metals (Ca^{2+}, Zn^{2+}, or Mn^{2+}).

Density functional theory (DFT) methods (for a review on quantum methods, see ref 29) were applied in conjunction with the Becke hybrid[30] (B3) exchange functional and the Lee−Yang−Parr (LYP)[31] correlation functional to study and characterize the above-mentioned metal-bound complexes, as there is wide agreement as to the adequacy of these methods to the study of this type of metal−ligand complex.[32,33] Full geometry optimization was carried out using the standard all-electron 6-31+G* basis set for the metal and effective core potentials and shared-exponent basis set of Stevens, Krauss, Basch, and Jasien (SBKJ),[34] including a polarization and a diffuse function for the ligands. This pseudopotentials/all-electron basis set combination was first found by N. Gresh et al.[35−37] to represent a well-balanced compromise between accuracy and computational efficiency and shall be denoted SBKJ+* hereafter. Vibrational frequencies were calculated at this level of theory to determine whether the obtained geometries correspond to a minimum on the potential energy surface (all frequencies are real). The energies were then refined by B3LYP/6-311++G(2df,2p) single-point calculations performed on the B3LYP/SBKJ+* geometries.

The changes in the Gibbs free energies of the reactions were calculated according to eq 3, where G, H, S, and T are the Gibbs free energy, enthalpy, entropy, and temperature ($T = 298$ K), respectively. The enthalpy can also be written as in eq 4:

$$\Delta G = \Delta H - T\Delta S \qquad (3)$$

$$H = E + RT = E_0 + E_{vib} + E_{rot} + E_{trans} + RT$$

$$= E_e + \text{ZPVE} + E_{vib} + E_{rot} + E_{trans} + RT \qquad (4)$$

where E_e, E_{vib}, E_{rot}, E_{trans}, and ZPVE are the electronic, therma, vibrational correction, rotational and translational energy components, and zero-point vibrational energies, respectively. Zero-point vibrational energies, thermal corrections to the energy (E_{vib}, E_{rot}, and E_{trans}) and entropies were calculated at the B3LYP/SBKJ+* level of theory, using standard statistical mechanical methods.[38] This method has been widely used in our group and has shown to be adequate for this type of calculations.[39−43]

Solvation Contributions. The environment is known to exert a substantial influence on the metal−ligand interaction energies.[10]

(29) Mercero, J. M.; Matxain, J. M.; Lopez, X.; York, D. M.; Largo, A.; Eriksson, L. A.; Ugalde, J. M. *Int. J. Mass Spectrom.* **2005**, *240*, 37−99.
(30) Becke, A. D. *J. Chem. Phys.* **1993**, *98*, 5648.
(31) Lee, C.; Yang, W.; Parr, R. G. *Phys. Rev. B* **1988**, *37*, 785.
(32) Labanowsky, J.; Andelzelm, J. *Density Functional Methods in Chemistry*; Springer-Verlag: New York, 1991.
(33) Alcamí, M.; Mo, O.; Yañez, M. *Mass Spectrosc. Rev.* **2001**, *20*, 195.
(34) Stevens, W. J.; Krauss, M.; Basch, H.; Jasien, P. G. *Can. J. Chem.* **1992**, *70*, 612.
(35) Garmer, D. R.; Gresh, N. *J. Am. Chem. Soc.* **1994**, *116*, 3556−3567.
(36) Gresh, N.; Stevens, W. J.; Krauss, M. *J. Comput. Chem.* **1995**, *16*, 843−855.
(37) Gresh, N.; Garmer, D. R. *J. Comput. Chem.* **1996**, *17*, 1481−1495.
(38) McQuarrie, D. A. *Statistical Mechanics*; Harper and Row: New York, 1976.
(39) Mercero, J. M.; Fowler, J. E.; Ugalde, J. M. *J. Phys. Chem. A* **1998**, *102*, 7006−7012.
(40) Mercero, J. M.; Fowler, J. E.; Ugalde, J. M. *J. Phys. Chem. A* **2000**, *104*, 7053−7060.
(41) Mercero, J. M.; Lopez, X.; Matxain, J. M.; Fowler, J. E.; Ugalde, J. M. *Int. J. Quantum Chem.* **2002**, *90*, 859−881.
(42) Mercero, J. M.; Mujika, J. I.; Matxain, J. M.; Lopez, X.; Ugalde, J. M. *Chem. Phys.* **2003**, *295*, 175−184.
(43) Mercero, J. M.; Matxain, J. M.; Rezabal, E.; Lopez, X.; Ugalde, J. M. *Int. J. Quantum Chem.* **2004**, *98*, 409−424.

Scheme 1. Thermodynamic Cycle Used to Compute the Free Energy of Binding of a Ligand to a Water-bound MIDAS Motif. ΔG^s_{M-W}, ΔG^s_{M-L}, ΔG^s_L and ΔG^s_W Are the Solvation Free Energies for the Water and Acetate-bound MIDAS Complexes, for the Different Ligands and for a Water Molecule, Respectively

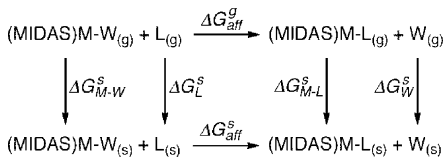

Table 1. Gas-Phase Affinity Energies (kcal/mol) of the Mg^{2+}-bound Closed and Open MIDAS Motif Toward an Acetate Decomposed in Its Various Components[a] for the Four Different MIDAS Models Studied

MIDAS conf.	ΔE_e	ΔE_0	ΔH_{298}	$T^*\Delta S_{298}$	ΔG^g_{aff}
$1S_{cl}$	−112.5	−110.4	−111.4	−4.2	−107.2
$1S_{op}$	−198.3	−199.2	−199.2	−2.6	−196.6
$2S_{cl}$	−115.2	−115.1	−115.4	−6.1	−109.3
$2S_{op}$	−119.9	−118.1	−119.1	−3.6	−115.5

[a] E_e = Total electronic energy; E_0 = zero-point corrected total electronic energy; H_{298} = enthalpy; S_{298} = entrophy; G_{298} = Gibbs free energy at 298 K.

Table 2. Comparison of ΔG Values (in kcal/mol) Obtained for the Open and the Closed MIDAS Conformations in the Ligand Binding Reaction at Different Dielectric Environments

solvent	ΔG^s_{aff} ($1S_{cl}$)	ΔG^s_{aff} ($1S_{op}$)	$\Delta\Delta G^s_{aff}$ ($1S_{op} - 1S_{cl}$)	ΔG^s_{aff} ($2S_{cl}$)	ΔG^s_{aff} ($2S_{op}$)	$\Delta\Delta G^s_{aff}$ ($2S_{op} - 2S_{cl}$)
gas phase	−107.2	−196.6	−89.4	−109.3	−115.5	−6.2
CCl_4	−49.3	−97.4	−48.1	−60.7	−65.5	−4.8
ether	−22.1	−52.2	−30.1	−39.0	−43.1	−4.1
acetone	−5.9	−23.8	−17.9	−26.9	−30.2	−3.3
water	8.9	−1.2	−10.1	0.8	−1.3	−2.1

Therefore, the effect of the surroundings of the MIDAS motif on its interaction with the ligand was evaluated doing single-point PCM calculations on the gas-phase geometries. The solvents used were the following: CCl_4 ($\epsilon = 2.2$), ether ($\epsilon = 4.3$), acetone ($\epsilon = 20.7$), and water ($\epsilon = 78.4$), which cover the dielectric environments ranging from completely buried regions in the protein to completely solvent-exposed ones.[44−46] To estimate the affinity energies in solution, the solvation free energy values (for each structure in each one of the solvents) were calculated and combined with the gas-phase affinity energies, as shown in Scheme 1.

All calculations were carried out with the GAUSSIAN98[47] package.

Results and Discussion

Affinity Regulated by Closed-to-Open Conformational Changes in the MIDAS Motif.

Affinity free energies of Mg^{2+}-bound $1S_{cl}$, $1S_{op}$, $2S_{cl}$, and $2S_{op}$ models for an acetate molecule were calculated according to eq 3. In Table 1, the gas-phase results obtained for each model, ΔG^g_{aff} (at 298 K), are decomposed into its various components: electronic energy (ΔE_e), electronic energy corrected by zero-point vibrational energies (ΔE_0), and enthalpy (ΔH_{298}) and entropy ($T^*\Delta S_{298}$) differences. In Table 2, solution phase results (ΔG^s_{aff}) are shown for the closed and open models, together with their relative affinity values, $\Delta\Delta G^s_{aff}(1S_{op} - 1S_{cl})$ and $\Delta\Delta G^s_{aff}$ ($2S_{op} - 2S_{cl}$), which were calculated according to eqs 5 and 6, respectively,

$$\Delta\Delta G^s_{aff}(1S_{op} - 1S_{cl}) = \Delta G^s_{aff}(1S_{op}) - \Delta G^s_{aff}(1S_{cl}) \quad (5)$$

$$\Delta\Delta G^s_{aff}(2S_{op} - 2S_{cl}) = \Delta G^s_{aff}(2S_{op}) - \Delta G^s_{aff}(2S_{cl}) \quad (6)$$

where $\Delta G^s_{aff}(1S_{op})$, $\Delta G^s_{aff}(1S_{cl})$, $\Delta G^s_{aff}(2S_{op})$, and $\Delta G^s_{aff}(2S_{cl})$ are the affinity energies for reaction 1, for the $1S_{op}$, $1S_{cl}$, $2S_{op}$, and $2S_{cl}$ structures, respectively. This is a measure of how the interaction of the MIDAS motif and an acetate molecule is modulated by the closed-to-open conformational change. Negative $\Delta\Delta G^s_{aff}$ values in Table 2 indicate that the open MIDAS conformation binds an acetate molecule with higher affinity than the closed conformation.

Gas-Phase Results. The gas-phase results (Table 1) for $1S_{cl}$ and $1S_{op}$, −107.2 and −196.6 kcal/mol, respectively, denote a high affinity of both conformations toward an acetate anion in the gas phase but much higher affinity of the open conformation ($\Delta\Delta G^s_{aff} = -89.4$ kcal/mol; Table 2). Analyzing the various contributions to the affinity energies in Table 1, we can observe that ΔG^g_{aff} values are mainly dominated by the electronic energies. Zero-point vibrational energy corrections, and the entropic terms in particular, tend, in general, to slightly decrease the affinity energies. The observed enhanced affinity of $1S_{op}$ toward an acetate molecule is likely due to the nature of the residues directly bound to the Mg^{2+} cation. The axial Asp-137 that is present in $1S_{cl}$ but is absent in $1S_{op}$ makes the total charge of the MIDAS change from +1 in $1S_{cl}$ to +2 in $1S_{op}$, which favors the interaction of the latter with a negatively charged acetate molecule, and, hence, a decrease (more negative) on ΔG^g_{aff} is observed.

Analysis of the X-ray structures of LFA-1 shows that the activation of the MIDAS from the closed to the open state is more accurately described as a displacement of Asp-137 from the first coordination shell to the second one with its substitution by a water molecule coming from the second coordination shell. Similarly, in the equatorial plane, there is an exchange between a water molecule and Thr-206. As was done for the 1S models of the MIDAS motif, the affinity energies for an acetate molecule were calculated for the 2S MIDAS models, according to eq 3. Data are also collected in Tables 1 and 2.

The effect of the second-shell ligands is more pronounced on the open MIDAS structures than on the closed ones. $2S_{cl}$ shows a moderate increase in the affinity for an acetate molecule (of around 2 kcal/mol) as compared to $1S_{cl}$. On the contrary, $2S_{op}$ shows a reduction in affinity of around 75 kcal/mol when compared to $1S_{op}$. The inclusion of second-shell ligands makes the net charge of $2S_{op}$ and $2S_{cl}$ the same (+1), provoking the affinity for an acetate molecule to become similar. However, although similar, the gas-phase affinity energies obtained for the $2S_{op}$ conformation are consistently larger (more negative) than those obtained for the closed conformations. The relative affinity free energy of $2S_{op}$ with respect to $2S_{cl}$ is −6.2 kcal/mol (Table 2). On the other hand, the trends of the different contributions to the gas-phase free energies is kept qualitatively similar (Table 1). Zero-point vibrational energy corrections tend to slightly decrease the affinity energy, and entropic contributions also lead to lower affinities. In this case, there is a significant contribution of the entropy to the differential affinity, as ca. 40% of the total relative affinity stems from the differential entropic factors between the $2S_{op}$ and $2S_{cl}$ models.

(44) Simonson, T. *J. Am. Chem. Soc.* **1998**, *20*, 4875−4876.
(45) Simonson, T.; Brooks, C. L. *J. Am. Chem. Soc.* **1995**, *118*, 8452−8458.
(46) Simonson, T.; Perahia, D. *Proc. Natl. Acad. Sci. U.S.A.* **1992**, *4*, 1082−1086.
(47) Frisch, M. J. et al., Gaussian 98, a.11; Gaussian, Inc., Pittsburgh, PA, **2001**.

Effect of the Dielectric Environment. In Table 2, the effect of different media on the affinity free energy (ΔG^s_{aff}) is shown. Solvation free energies for each of the structures that characterizes the closed and open states of the MIDAS, $1S_{op}$, $1S_{cl}$, $2S_{op}$, and $2S_{cl}$ in the acetate-bound or acetate-unbound form, as well as for an acetate and a water molecule individually, were calculated. The results of the calculations show that the solvation free energies were modulated by the total charge of the structure, the volume of the structure, and the dielectric permittivity of the environment in the following way: the larger the charge, the smaller the volume and the more polar the environment, the larger the solvation free energy of the structure (Table S3 in Supporting Information). These energies were combined with the gas-phase affinity free energies to give the total affinity free energy in solution according to Scheme 1.

In general, more polar environments led to a lower affinity of the MIDAS toward an acetate (i.e., less negative values in Table 2) and to a smaller affinity difference between closed and open structures. In the most extreme case, that of $\epsilon = 78.4$ (water), positive values of the affinity energies were found for the closed structures: 8.9 kcal/mol for $1S_{cl}$ and 0.8 kcal/mol for $2S_{cl}$. These effects are due mainly to the partial charge neutralization upon ligand binding (leading to a lower solvation free energy) combined with the unfavorable desolvation of the acetate.

The relative affinity for an acetate molecule between the closed and open conformations ($\Delta\Delta G^s_{aff}$ in Table 2), for 1S and 2S MIDAS models, is also highly affected by the polarity of the media. The more polar the environment, the lower the values of $\Delta\Delta G^s_{aff}$. That is, $\Delta\Delta G^s_{aff}$ is reduced (in absolute value) from -89.4 in the gas phase to -10.1 kcal/mol in water for the 1S MIDAS models and from -6.2 to -2.1 kcal/mol for the 2S models. As the solvent polarity increases, there is a reduced influence of the second coordination shell residues on the open/closed MIDAS relative affinity energies. For instance, in low-dielectric environments (CCl_4), there is a substantial difference between $\Delta\Delta G^s_{aff}(1S_{op} - 1S_{cl})$ and $\Delta\Delta G^s_{aff}(2S_{op} - 2S_{cl})$, -48.1 vs -4.8 kcal/mol, whereas in water these differences are reduced (-10.1 vs -2.1 kcal/mol). Nevertheless, regardless of the model used for the MIDAS, we find that low-dielectric media favor affinity of the MIDAS toward the glutamate-like ligand and also favor the affinity of the open states with respect to the closed ones. These results explain the fact that the MIDAS site in the I-domain of LFA-1 is surrounded by a hydrophobic environment that ensures a low-dielectric permittivity and, hence, more efficient coordination of the metal with the carboxylate of the ligand.[8] Moreover, the large effect exerted by second-shell ligands or apolar environments around the MIDAS has important implications in drug design and points to the use of an acetate-type functional group surrounded by hydrophobic substituents as a putative nonallosteric model inhibitors of the LFA-1/ICAM-1 interaction. In summary, our results show that fundamental characteristics of ligand binding by the MIDAS of the I-domain are governed by the changes in conformation around the metal ion and the hydrophobic environment provided by surrounding residues.

Replacement of Cations in the MIDAS. Is the interchange between Zn^{2+}, Ca^{2+}, or Mn^{2+} and Mg^{2+} in the MIDAS motif thermodynamically favorable? To address this question, reactions depicted in Scheme 2 were studied with the MIDAS in

Scheme 2. Representation of the Reactions of Metal Exchange for the Closed (left) and Open (right) MIDAS Motif

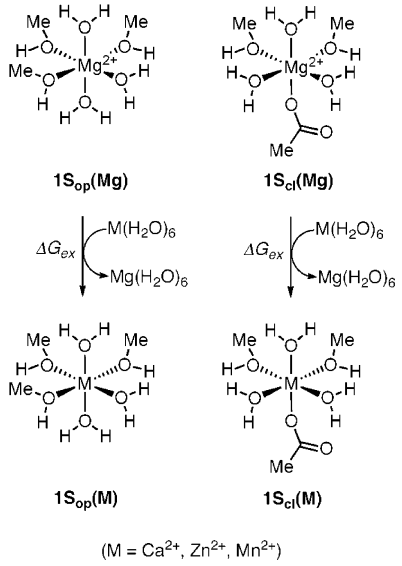

the two alternative conformations: $1S_{cl}$ and $1S_{op}$. This one-shell model was chosen because the precedent calculations showed no qualitative variations on passing from the one-shell model to the two-shell model, but it had the advantage of being more sensitive to variations around the MIDAS. Concerning the preferred coordination of each of the cations under study, an octahedral geometry has been observed for solvated Ca^{2+}, Mg^{2+}, Zn^{2+}, and Mn^{2+} and for protein-bound Mg^{2+} and Mn^{2+}.[7,48,49] The coordination number for the Ca^{2+} cation ranges from 6 to 8 in proteins,[48] whereas for the Zn^{2+} cation, the coordination number depends on its role. In enzymes, where the zinc ion is often bound to Glu and His residues, a distorted square pyramidal coordination is usually observed, whereas it adopts a tetrahedric coordination when it plays a structural role[50,51] and is often found bound to Cys residues. In some proteins, a coordination number of six has also been observed.[49,51] We emphasize that in every reaction studied in the present work, the incoming metal retains the coordination geometry of the outgoing metal. Regarding the spin multiplicity on Mn^{2+} octahedral complexes, only the high-spin structures will be discussed.[52] Values for ΔG_{ex} can be found in Table 3.

When including the effect of the polarity of the environment, we must take into account that the hexahydrated compounds represent fully solvated cations. Therefore, the solvation free energy for these structures was only evaluated in water-like environments. The MIDAS motif can still be exposed to media with different polarities, and therefore, various possibilities have been considered in Table 3.

(48) Katz, A. K.; Glusker, J. P.; Beebe, S. A.; Bock, C. W. *J. Am. Chem. Soc.* **1996**, *118*, 5752−5763.
(49) Glusker, J. P.; Katz, A.; Bock, C. W. *Rigaku J.* **1999**, *16*, 8−16.
(50) Marcus, Y. *Chem. Rev.* **1988**, *88*, 1475−1498.
(51) Alberts, I. L.; Nadassy, K.; Wodak, S. J. *Protein Sci.* **1998**, *7*, 1700−1716.
(52) It is usual to assume that the Mn^{2+} complexes in proteins are high-spin molecules, and such an assumption has been widely used in almost every work concerning these types of complexes.[63,64] In this study, high (IV)- and low (II)-spin Mn^{2+} complexes have been studied. We have found that, as expected, the Mn^{2+} structures with water ligands are high-spin complexes, the electronic energy difference between high-spin and low-spin states being 7.0 kcal/mol. Similarly, for the acetate-bound or acetate-unbound Mn^{2+} open MIDAS motifs, the most stable molecules are high-spin complexes, with an electronic energy difference of 13.1 and 18.0 kcal/mol, respectively. As a consequence, we decided to use the high-spin complexes for every reaction discussed in this work in which the Mn^{2+} cation was involved.

Table 3. ΔG_{ex} (kcal/mol) Calculated for the Cations Exchange Reactions Prior to Ligand Binding at Different Dielectric Environments

	$1S_{cl}$			$1S_{op}$		
solvent	Zn^{2+}	Ca^{2+}	Mn^{2+}	Zn^{2+}	Ca^{2+}	Mn^{2+}
gas phase	−2.2	9.1	−8.6	−1.6	1.3	−5.3
CCl_4	−2.7	0.7	−9.8	−4.2	−3.5	−4.5
ether	−2.2	1.5	−9.0	−3.8	−1.9	−3.3
acetone	−2.3	2.6	−11.0	−3.9	−0.3	−3.3
water	−1.1	4.1	−3.2	−2.4	7.3	2.3

Our results indicate an interesting dependence of metal exchange energy on the conformation of the MIDAS and nature of the metal. In the case of Zn^{2+}, negative values of ΔG_{ex} are obtained regardless of the conformation of the MIDAS, closed or open, or of the polarity of the environment. The exchange energies range from −1.1 (water-like permittivity) to −2.2 kcal/mol (gas phase) for the $1S_{cl}$ structure. For the open conformation $1S_{op}$, ΔG_{ex} are negative as well, but they are consistently higher in absolute value than for $1S_{cl}$, ranging from −2.4 (water) to −1.6 kcal/mol (gas phase). In any case, these energies reveal that displacement of Mg^{2+} by Zn^{2+} would be possible in an octahedric open or closed MIDAS motif.

On the other hand, and according to our results, exchange possibilities for the Ca^{2+} cation strongly depend on the conformation of the MIDAS. When the MIDAS is in its closed conformation,[53] $1S_{cl}$(Mg), positive values for the ΔG_{ex} energies are obtained, which range from 4.1 in water to 9.1 kcal/mol in the gas phase. These values indicate that the displacement of Mg^{2+} by Ca^{2+} in the closed MIDAS is thermodynamically unfavorable. However, in the case of the open MIDAS conformation, $1S_{op}$(Mg), with the metal surrounded by all formally neutral ligands, there are some permittivity values of the media, such as those modeled by the solvents CCl_4 and ether, for which a negative value of the exchange energy is found, −3.5 and −1.9 kcal/mol, respectively. In addition, for acetone, we also get a negative value, −0.7 kcal/mol, but because this number is lower than 1 kcal/mol in absolute value, we may consider this reaction as thermoneutral. Taking into account these data, it appears that the closed MIDAS conformation inhibits the displacement of Mg^{2+} by Ca^{2+}, whereas the probability for Mg^{2+}/Ca^{2+} exchange in the open MIDAS motif strongly depends on the surroundings. Interestingly, when the optimized metal−MIDAS geometries were compared (see Supporting Information), one observes that the geometry of the Ca^{2+}-bound MIDAS changed more significantly than the others, suggesting that Ca^{2+} may prefer to coordinate to a higher number of ligands; this, in turn, would result in a significant structural rearrangement of the surroundings.

On the contrary, exchange between Mg^{2+} and Mn^{2+} is favorable, regardless of the conformation of the MIDAS motif and the dielectric permittivity of the environment. When the MIDAS is in the closed conformation, exchange energies range from −8.6 in the gas phase to −3.2 kcal/mol in water. The metal exchange in the open MIDAS conformation is also favored for all the permittivity values tested except for that of water. The ΔG_{ex} values range from −5.3 in a vacuum to 2.3 kcal/mol in water. Then, it seems that the replacement of Mg^{2+} by Mn^{2+} is favored for both MIDAS conformations and for either polar or more-hydrophobic environments (except water).

(53) Because of the geometric and electronic features of the MIDAS, we have restricted our analysis to octahedral geometries for Ca^{2+}, although other configurations for this cation have been described.[48] Further work is in progress to study the possible effects in MIDAS of integrins by different coordination patterns.

Scheme 3. Representation of the Ligand Binding Reaction for the Open MIDAS Motif, With Different Metals as Central Cations

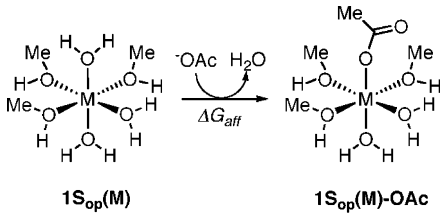

Affinity Regulated by the Metal Cation. The affinity energies toward an acetate ligand were evaluated for the $1S_{op}$ conformation of the MIDAS and with Ca^{2+}, Zn^{2+}, and Mn^{2+} as the central metal cation.

Gas-Phase Results. Gas-phase affinity energies toward an acetate of the $1S_{op}$ MIDAS structures with different metal cations (Scheme 3) are collected in Table 4. The ΔG^{s}_{aff} values obtained with each metal are shown along with the relative $\Delta\Delta G^{s}_{aff}$ values with respect to Mg^{2+}. The four cations show negative values of ΔG^{s}_{aff}; i.e., the coordination to an acetate molecule and the displacement of a water molecule are thermodynamically favorable for all metals tested. However, there are sizable and consistent differences among the affinity results obtained for each cation. The Ca^{2+}-bound open MIDAS motif shows lower affinity energies than the Mg^{2+}-bound open MIDAS, whereas the presence of Zn^{2+} or Mn^{2+}(IV) in the open MIDAS motif increases the affinity toward an acetate. For the Zn^{2+}-bound open MIDAS, the improvement is moderate, whereas Mn^{2+}(IV) provokes a considerable enhancement of the affinity energy compared to the Mg^{2+}-bound open MIDAS.

Effect of the Dielectric Environment. Solvent effects are qualitatively similar in all three cases: the more polar the solvent is, the lower individual affinity energies are (data not shown). In general, there is also a decrease in the relative affinities with respect to magnesium with polarity of the media, leading to lower absolute values of $\Delta\Delta G^{s}_{aff}$, with the only exception of $\Delta\Delta G^{s}_{aff}$(Zn−Mg) in water solvent.

Overall, our results suggest that (i) the presence of Zn^{2+} or Mn^{2+} on the MIDAS motif is compatible with an octahedric coordination, whereas (ii) the coordination number of the Ca^{2+} cation may increase in either the open or closed MIDAS motif; (iii) a Ca^{2+} cation bound to the octahedral open MIDAS motif would have a decreased affinity for the ligand relative to Mg^{2+}-bound open MIDAS motif; (iv) a Zn^{2+} cation would, albeit slightly, increase the affinity of the MIDAS motif for a carboxylic side chain, and (v) a Mn^{2+} cation would considerably increase the affinity of the MIDAS motif for a carboxylic side chain.

In experiments with isolated I-domains of the integrins LFA-1 and MAC-1,[17] it has been shown that Zn^{2+} and Mn^{2+} can bind to both I-domains (with equivalent closed and open MIDAS motives). In addition, it is well-known that Zn^{2+} can compete with Mg^{2+} in other metal binding sites.[54−57] Our geometry optimizations indicate that the octahedral coordination of the MIDAS site would be maintained in the presence of Zn^{2+}. Moreover, our data indicate that a Zn^{2+}-coordinating MIDAS

Table 4. Affinity Differences (kcal/mol) of the Ca^{2+}- and the Zn^{2+}-Bound Open MIDAS toward an Acetate Molecule, With Respect to the Mg^{2+}-Bound Open MIDAS, and at Different Dielectric Environments

	ΔG_{aff}				$\Delta\Delta G_{aff}$		
solvent	Mg^{2+}	Zn^{2+}	Ca^{2+}	Mn^{2+}	$\Delta\Delta G_{Mg}^{Zn}$ [a]	$\Delta\Delta G_{Mg}^{Ca}$ [b]	$\Delta\Delta G_{Mg}^{Mn}$
gas phase	−196.6	−198.9	−187.0	−203.5	−2.3	9.6	−6.9
CCl_4	−97.4	−99.4	−92.7	−97.4	−2.0	4.7	−6.6
ether	−52.2	−53.9	−49.0	−58.5	−1.7	3.2	−6.3
acetone	−23.8	−25.5	−22.2	−30.5	−1.4	1.6	−6.7
water	−1.2	−6.1	−0.3	−6.9	−4.6	0.9	−5.7

[a] Computed as $\Delta\Delta G_{Mg}^{Zn} = \Delta G_{aff}^{s}(Zn - MIDAS) - \Delta G_{aff}^{s}(Mg - MIDAS)$. [b] Computed as $\Delta\Delta G_{Mg}^{Ca} = \Delta G_{aff}^{s}(Ca - MIDAS) - \Delta G_{aff}^{s}(Mg - MIDAS)$.

Table 5. Comparison of ΔG_{aff}^{s} Values (kcal/mol) Obtained for the Open MIDAS Conformations with Various Ligands and in Different Model Solvents[a,b]

solvent	1a	1b	1c	1d	1e	1f	1g	1h	2a	2b
gas phase	−192.9	−196.6	−195.4	−195.2	−175.2	−173.5	−172.0	−189.6	−191.5	−194.6
	(+**3.7**)	(**0.0**)	(+**1.2**)	(+**1.4**)	(+**21.4**)	(+**23.1**)	(+**24.6**)	(+**7.0**)	(+**5.1**)	(+**2.0**)
CCl_4	−94.2	−97.4	−96.7	−96.9	−83.1	−81.7	−80.6	−92.4	−94.9	−97.6
	(+**3.2**)	(**0.0**)	(+**0.7**)	(+**0.5**)	(+**14.3**)	(+**15.7**)	(+**16.8**)	(+**5.0**)	(+**2.5**)	(−**0.2**)
ether	−50.4	−52.2	−51.6	−52.1	−43.3	−41.1	−41.8	−47.8	−51.4	−53.8
	(+**1.8**)	(**0.0**)	(+**0.6**)	(+**0.1**)	(+**9**)	(+**11.1**)	(+**10.4**)	(+**4.4**)	(+**0.8**)	(−**1.6**)
acetone	−22.8	−23.8	−23.8	−24.0	−17.0	−17.9	−14.9	−20.7	−23.9	−26.3
	(+**1.0**)	(**0.0**)	(**0.0**)	(−**0.2**)	(+**6.8**)	(+**5.9**)	(+**8.9**)	(+**3.1**)	(−**0.1**)	(−**2.5**)
water	−0.6	−1.2	−0.5	−1.1	1.3	4.5	6.3	−1.0	−3.8	−3.9
	(+**0.6**)	(**0.0**)	(+**0.7**)	(+**0.1**)	(+**2.5**)	(+**5.7**)	(+**7.5**)	(+**0.2**)	(−**2.6**)	(−**2.7**)

[a] In parenthesis, the relative affinity ($\Delta\Delta G_{aff}^{s}$) with respect to the affinity showed toward an acetate, i.e., $\Delta\Delta G_{aff}^{s}(ligand) = \Delta G_{aff}^{s}(ligand) - \Delta G_{aff}^{s}(acetate)$, calculated at different dielectric environments. [b] 1a = formate; 1b = acetate; 1c = propionte; 1d = butirate; 1e/1f/1g = TriF/TriCl/TriBr−acetate; 1h = benzoate; 2a = nitromethene; 2b = nitropropene.

site would have a similar affinity for acetate as a Mg^{2+}-bound MIDAS site.

It has also been shown that Mn^{2+} can substitute Mg^{2+} in several metalloproteins, including LFA-1.[17] In several cases, this substitution is associated with substantial increase in binding affinities.[17,58−60] Our calculations on the model system indicate that not only can Mn^{2+} substitute Mg^{2+} as the metal coordinating cation, but that it would substantially increase the affinity of the open MIDAS motif for an acetate.

On the other hand, as mentioned above, Ca^{2+} cation has shown controversial results in similar integrins. In the experiments mentioned above with isolated I-domains,[17] Ca^{2+} cation seemed to bind to Mac-1 but not to LFA-1. Our data indicate that structural rearrangements of the MIDAS may take place upon Ca^{2+} binding, as the optimized geometry of the Ca^{2+}-bound MIDAS changed the most, compared to those geometries with other metal cations. The different abilities of Ca^{2+} to bind equivalent MIDAS motifs, might be related to protein flexibility around the MIDAS, which may allow conformational rearrangements in LFA-1 but not in Mac-1. However, the importance of Mn^{2+} and Ca^{2+} cations in integrin activation via the adjacent to metal-ion-dependent site (ADMIDAS) of I-like domains of β subunits must also be taken into account.[61]

Scheme 4. Representation of the Reactions Studied and the Ligands Tested: 1a = Formate; 1b = Acetate; 1c = Propionte; 1d = Butirate; 1e = Benzoate; 1f/1g/1h = TriF/TriCl/TriBr−acetate; 2a = Nitromethene; 2b = Nitropropene

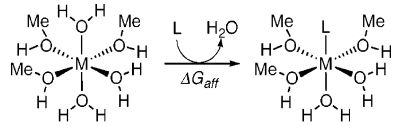

$1S_{op}$(Mg) **$1S_{op}$(Mg)-L**

(L=**1a-h**, **2a,b**)

1

1a: R^1=H **1e**: R^1=CF_3
1b: R^1=CH_3 **1f** : R^1=CCl_3
1c: R^1=CH_2CH_3 **1g**: R^1=CBr_3
1d: R^1=$CH_2CH_2CH_3$ **1h**: R^1=C_6H_5

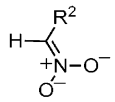

2

2a: R^2=H
2b: R^2=$CH_2CH_2CH_3$

Affinity for Different Types of Ligands. To design novel inhibitory drugs, it is necessary to study the affinity energies of the MIDAS toward different ligands or substrates. In this spirit, the affinity energy of the open MIDAS structure $1S_{op}$ was evaluated for 10 different ligands. The reactions studied and the tested ligands are shown in Scheme 4, and the results are found in Table 5.

The affinity values obtained for the formate (1a), acetate (1b), propionate (1c), and butyrate (1d) molecules are compared first. These four molecules differ on the length of the aliphatic chain

(54) Ciancaglini, P.; Pizauro, J. M.; Curti, C.; Tedesco, A. C.; Leone, F. A. *Int. J. Biochem.* **1990**, *22*, 747−751.
(55) Lukat, G. S.; Stock, A. M.; Stock, J. B. *Biochemistry* **1990**, *29*, 5436−5442.
(56) Sun, L.; Martin, D. C.; Kantrowitz, E. R. *Biochemistry* **1999**, *38*, 2842−2848.
(57) Lee, L. V.; Poyner, R. R.; Vu, M. V.; Cleland, W. W. *Biochemistry* **2000**, *39*, 4821−4830.
(58) Leupold, C. M.; Goody, R. S.; Wittinghofer, A. *Eur. J. Biochem.* **1983**, *135*, 237−241.
(59) Wittinghofer, A.; Leberman, R. *Eur. J. Biochem.* **1979**, *93*, 95−101.
(60) Schweins, T.; Scheffezek, K.; Assheuer, R.; Wittinghofer, A. *J. Mol. Biol.* **1997**, *266*, 847−856.
(61) Chen, J.; Takagi, J.; Xie, C.; Xiao, T.; Luo, B.-H.; Springer, T. A. *J. Biol. Chem.* **2004**, *279*, 55556−55561.

bound to the carboxylate, and they can be taken as probes of the sensitivity of the ligand toward substituents with increased electron σ-donor capability. ΔG^{s}_{aff} values in the gas phase are similar for all of them but lower for the formate (−192.9, −196.6, −195.4, and −195.2 kcal/mol, respectively, for increasing chain length). This similarity is also observed in water ($\Delta G^{s}_{aff} = -0.6, -1.2, -0.5$, and −1.1 kcal/mol, respectively). An inspection of the relative affinity values with respect to acetate in Table 5 (in parentheses) shows that formate is not as good of a ligand as acetate; the $\Delta\Delta G^{s}_{aff}$ ranges from 3.7 in the gas phase to 0.6 in water, whereas the values for propionate and butyrate are in general within 1 kcal/mol of the value for acetate. Hence, it can be concluded that beyond the length of an acetate molecule, the increased electron σ-donor character of the aliphatic chain has a minor effect on the affinities. Therefore, selectivity toward an aspartate or glutamate amino acid side chain in the integrin might be determined by the complementary shape of the surroundings of the MIDAS with the vicinity of residues of the natural ligand. Springer et al.[62] have found experimentally that the binding affinity of I-domain of α_X subunit follows the trend acetate > propionate > formate, in nice agreement with our computational results on the α_L subunit.

Considered next are ligand substitutions that provoke an electron σ-acceptor inductive effect. For this purpose, the affinity energies for trifluoro-, tricloro-, and tribromo-acetate ligands (Scheme 4: 1e, 1f. and 1 g, respectively) were calculated. Interestingly, they all show lower affinity energies with respect to acetate. In vacuo, the relative affinity values with respect to acetate are 21.4, 23.1, and 24.7 kcal/mol, respectively, indicating a substantial decrease in binding capability. When different permittivity values are considered, the above-mentioned differences decrease, but they are all maintained at considerable positive values (2.5, 5.7, and 7.5 kcal/mol, respectively, in water). These results suggest that the presence of substituents with significant σ-acceptor character will lead to a ligand with a lower capacity of electron donation to the metal center and, therefore, with a lower binding affinity.

In line with these results, a benzoate ligand (Scheme 4: 1h) was tested, which stabilizes the electronic charge of the ligand by a π resonance, and was found to be a ligand that leads to lower affinity energies than the ones showed by the reference acetate ligand. The ΔG^{s}_{aff} values range from −189.6 in the gas phase to −1.0 kcal/mol in water. From these results, we can conclude that the design of inhibitors of the LFA-1/ICAM-1 interaction should include carboxylic acids in their metal binding moiety, but electron withdrawing groups (alfa-halo carboxy donors) or aromatic rings (benzoates or heteroaromatic analogues) should be avoided. On the other hand, these alkyl carboxylate groups must be surrounded by a hydrophobic environment to lower the effective ϵ value around Mg^{2+}, thus increasing the binding ability of the MIDAS.

Finally, we also checked the behavior toward negatively charged nitronate ligands (2a and 2b). Affinity values for these ligands were in the same range as for formate and acetate molecules. Furthermore, for nitropropene in a polar media, affinity values were found that were higher than those for acetate. This suggests that nitro functional groups could be promising substituents of the carboxylate as the protruding group in this sort of ligand without compromising their binding capabilities to the MIDAS.

Conclusions

The various factors that contribute to the binding energy of integrins and their ligands, such as the nature and coordination of the metal, the activation state of the protein, the nature of the ligand, or the experimental conditions make it difficult to determine experimentally the relative contributions of each individual phenomena; this can be the source of the controversial results in some of these works. In this study, we present the results of quantum calculation on a realistic model of the metal-ion-dependent adhesion site (MIDAS) of the integrin LFA-1 that significantly help to understand different aspects of the affinity modulating mechanisms of the interaction between the MIDAS motif and key residues in its counter-receptor ICAM-1 (such as E34). This has been accomplished by individually studying the isolated effect on the ligand binding affinity of the different factors mentioned above.

Concerning the two possible coordination modes of the MIDAS motif, we have (i) quantified the change (gain) in ligand affinity related to the closed to open conformational change in the MIDAS motif, observing that the open MIDAS binds E34 of ICAM-1 with a higher affinity than the closed MIDAS. A major point in this respect is that the surroundings of the MIDAS motif contribute to the regulation of the affinity toward the ligand as much as or to a higher extent than the conformational change mentioned above. In this respect, we have found that the inclusion of second-shell ligands in the MIDAS model dramatically decreases the differences in ligand affinity and that hydrophobic environments (low-dielectric value) around the MIDAS and the approaching acetate molecule dramatically increase the strength of this interaction. This behavior helps to understand why the MIDAS motif has only been observed in its open state when bound to ICAM-1, and (ii) the Mg^{2+} ion in the MIDAS and the anionic E34 residue in ICAM-1 are mainly surrounded by hydrophobic residues in the protein.

Our conclusions related to the effect of the different metals (Mg^{2+}, Zn^{2+}, Ca^{2+}, and Mn^{2+}) help to clarify the controversial experimental results obtained for the role of these metals on ligand-binding activity of integrins. This controversy may arise from the difficulty in isolating the intrinsic effect of the metals from many other factors that affect ligand binding activity in integrins, as stated by Ajroud et al.[22] From our results, we observed that Mg^{2+} may be the most abundant but not necessarily the best cation for the purposes of entering the MIDAS and strongly binding to ICAM-1. Other ions, such as Zn^{2+} and especially Mn^{2+} (IV), could coordinate to the MIDAS motif and substantially favor ICAM-1 binding. On the other hand, too-strong bindings are not necessarily desired from a physiological point of view, as there must eventually be a release of ligand at a certain point of the biological process taking place. On the contrary, the inhibitory effect of the Ca^{2+} cation may be due to the fact that it is not easily accommodated in an octahedral geometry of the MIDAS, and its binding may lead to a structural distortion of the MIDAS and the surrounding environment.

(62) Vorup-Jensen, T.; Carman, C. V.; Shimaoka, M.; Schuck, P.; Svitel, J.; Springer, T. A. *Proc. Natl. Acad. Sci. U.S.A.* **2005**, *102*, 1614−1619.
(63) Siegbahn, P. E. M. *Theor. Chem. Acc.* **2001**, *105*, 197−206.
(64) Waizumi, K.; Ohtaki, H.; Masuda, H.; Fukushima, N.; Watanabe, Y. *Chem. Lett.* **1992**, *8*, 1489−1492.

Concerning the synthesis of new inhibitors of the LFA-1/ICAM-1 interaction, we concluded that carboxylic acids included in the metal-binding moiety would improve the affinity for the LFA-1 I-domain, whereas electron-withdrawing groups (alfa-halo carboxy donors) or aromatic rings (benzoates or heteroaromatic analogues) should be avoided because they lead to lower binding affinities. On the contrary, nitronates surrounded by hydrophobic groups, may yield binding affinities as good as or even better than the carboxylic acids. Interestingly, we observed that there is no direct correlation between the capacity of the ligands to donate charge to the metal and the increase in their affinity toward the MIDAS (paper in preparation).

Acknowledgment. This work was supported by Universidad del Pais Vasco/Euskal herriko Unibertsitatea and Eusko Jaurlaritza (Grant 9/UPV000170.215-13548/2001) and by Spanish Ministerio de Educacion y Ciencia (Projects BQU2001-0904 and CTQ2004-06816/BQU). The SGI/IZO-SGIker UPV/EHU (supported by the National Program for the Promotion of Human Resources within the National Plan of Scientific Research, Development, and Innovation − Fondo Social Europeo and MCyT) is gratefully acknowledged for generous allocation of computational resources in Spain. Support from the Centre National de la Recherche Scientifique (A.D., R.H.S.), the Institut National de la Santé et de la Recherche Médicale (A.D.), and the Université Louis Pasteur de Strasbourg (A.D., R.H.S.) are gratefully acknowledged. Computational resources in France were provide by the Centre Informatique National de l′Enseignement Supérieur (CINES) and the Institut du Dévelopement et des Ressources en Informatique Scientifique (IDRIS-CNRS). The collaborative nature of this work is supported, in part, by EGIDE and the Ministère des Affaires Etrangéres, France.

Supporting Information Available: ΔG^{g}_{aff} values for the acetate binding reaction of the Mg^{2+}-, Ca^{2+}-, and Zn^{2+}-bound $1S_{op}$ MIDAS models were calculated at three different levels of theory to calibrate our method, and data are collected in the Supporting Information. Computed and experimental metal−oxygen distances and complete refs 24, 27, and 47 can also be found as Supporting Information. This material is available free of charge via the Internet at http://pubs.acs.org.

JA054142A